Anand Balu Nellippallil
Aerospace and Mechanical Engineering,
University of Oklahoma,
Norman, OK 73019
e-mail: anand.balu@ou.edu

Vignesh Rangaraj
Industrial and Systems Engineering,
University of Oklahoma,
Norman, OK 73019
e-mail: rangaraj.vignesh@ou.edu

B. P. Gautham
TCS Research,
54-B, Hadapsar Industrial Estate,
Pune 411013, Maharashtra, India
e-mail: bp.gautham@tcs.com

Amarendra Kumar Singh
Materials Science and Engineering,
Indian Institute of Technology Kanpur,
Kanpur 208016, India
e-mail: amarendra@iitk.ac.in

Janet K. Allen[1]
School of Industrial and Systems Engineering,
202 W Boyd Street, Room 116-G,
University of Oklahoma,
Norman, OK 73019
e-mail: janet.allen@ou.edu

Farrokh Mistree
Aerospace and Mechanical Engineering,
University of Oklahoma,
Norman, OK 73019
e-mail: farrokh.mistree@ou.edu

An Inverse, Decision-Based Design Method for Integrated Design Exploration of Materials, Products, and Manufacturing Processes

A material's design revolution is underway with a focus to design the material microstructure and processing paths to achieve certain performance requirements of products. A host of manufacturing processes are involved in producing a product. The processing carried out in each process influences its final properties. To couple the material processing-structure-property-performance (PSPP) spaces, models of specific manufacturing processes must be enhanced and integrated using multiscale modeling techniques (vertical integration) and then the input and output of the various manufacturing processes must be integrated to facilitate the flow of information from one process to another (horizontal integration). Together vertical and horizontal integration allows for the decision-based design exploration of the manufacturing process chain in an inverse manner to realize the end product. In this paper, we present an inverse method to achieve the integrated design exploration of materials, products, and manufacturing processes through the vertical and horizontal integration of models. The method is supported by the concept exploration framework (CEF) to systematically explore design alternatives and generate satisficing design solutions. The efficacy of the method is illustrated for a hot rod rolling (HRR) and cooling process chain problem by exploring the processing paths and microstructure in an inverse manner to produce a rod with specific mechanical properties. The proposed method and the exploration framework are generic and support the integrated decision-based design exploration of a process chain to realize an end product by tailoring material microstructures and processing paths. [DOI: 10.1115/1.4041050]

1 Frame of Reference

Steel manufacturers focus on developing new grades of steels with improved properties and performance. Careful managing of material processing during steel manufacturing will lead to the development of steels with a range of mechanical properties resulting in the improved performance of products. A round rod is produced after passing the raw steel through several manufacturing processes such as casting, reheating, rolling, and cooling. This round rod forms the input material for gear production. The chemical composition of the steel including the segregation of alloying elements, the deformation history during rolling, the cooling after rolling, and the microstructure generated define the end properties of the rolled product. The presence of large numbers of design variables, constraints and bounds, conflicting goals, and sequential information/material flow during material processing makes the steel rod making process chain highly complex. Many plant trials are therefore required to produce a new steel grade with desired properties and performance. These trials are usually expensive and time-consuming. An alternative is to carry out simulation-based, integrated design exploration of the different manufacturing processes involved in exploiting the advances in computational modeling and identifying a ranged set of solutions that satisfy the requirements both of the steel manufacturing process and the end rod product.

In practice, design is involved with the selection of a suitable material for a given application. The classical material selection approaches are being replaced by a materials design revolution that is underway in the recent past where the focus is to design the material microstructure or mesostructure to achieve certain performance requirements such as density, strength, ductility, toughness, and hardness. The demands on the microstructure placed by these multiple performance requirements are often in conflict.

Our interest lies in formulating and solving the inverse problem: given the required end properties/performance, what should be the input parameters in terms of material microstructure and processing paths for the model-based realization of the material, product, and the manufacturing processes?

From a system's design perspective, we view design as a *top-down, simulation-supported, integrated, decision-based process to satisfy a ranged set of product-level performance requirements* [1,2]. Keeping with this and the discussions by Olson on materials-by-design [3], we view the integrated design of materials, products, and processes as *fundamentally an inverse, goal-oriented synthesis activity in which the designer (decision-maker) aims at identifying material structures and processing paths that achieve/satisfy certain required product and process-level properties and performances*. From the standpoint of design community, design process is always the inverse process of identifying design variables to realize desired properties or performances. However,

[1]Corresponding author.

Contributed by the Design Automation Committee of ASME for publication in the Journal of Mechanical Design. Manuscript received March 1, 2018; final manuscript received July 19, 2018; published online September 7, 2018. Assoc. Editor: Yan Wang.

the word "inverse" is used here from the perspective of materials design community and will be explained in the sections that follow.

The philosophical underpinning of the goal-oriented approach to materials design has been provided by Olson [3] and reiterated by many others [2,4–6]. The conventional way of modeling hierarchical processes and systems is a "bottom-up," cause and effect (deductive) approach of modeling the material's processing paths, microstructures, resulting properties, and then mapping the property relations to performance functions, as shown in Fig. 1. Over the years, the focus in materials design has turned to provide high-throughput decision support and develop inverse methods for materials design exploration as discussed by McDowell and Kalidindi [7]. There are several works in this vein. Adams et al. [8] present a framework that utilizes highly efficient spectral representations to arrive at invertible linkages between material structure, its properties, and the processing paths used to alter the material structure. The materials knowledge systems approach by Kalidindi et al. [9] and [10] showcase advances in rapid inverse design to estimate local responses. However, all these approaches including the strategy proposed by McDowell and Olson [11] fall to specific classes of materials design problems and demands considerable knowledge and insight in mechanisms, material hierarchy and information flow. Thus, these classes of inverse design approaches are mostly suited for detailed design and not for "design exploration" [5].

In our work, we seek "top-down," goals/means, inductive, or inverse methods especially at early stages of design to explore the design space of processing paths and resulting microstructures of a material *satisfying* a set of specified performance requirements, see Fig. 1. Approaches to pursue top-down design exploration by employing multiscale modeling and systems-based design especially at early stages of design are addressed in limited literatures. Choi et al. [12,13] propose the inductive design exploration method (IDEM); a multilevel, robust design method that makes it possible to consider propagation of all three types of uncertainty [14], such as that arising in hierarchical materials design problems that incorporates process-structure-property (SP) relations. The two major design objectives using the IDEM for material and product design are [11]: (i) to guide bottom-up modeling so as to conduct top-down, goal-oriented design exploration, (ii) to manage the uncertainty in chains of process-structure-property relations. Kern et al. [15] propose pyDEM a generalized implementation of the IDEM as an open-source tool in the Python environment. The top-down, goal-oriented approach of materials design comes with several challenges as highlighted by McDowell et al. [16]. In this paper, we address the challenge of incorporating the design of the material as part of a larger overall systems design process embodying the hierarchy of process-structure-property-performance set forth by Olson [3] with consideration on supporting coordination of information and human decision-making.

To carry out design space exploration across the material processing-structure-property-performance (PSPP) spaces, there should be flow of information via simulation models integrated across multiple scales and across multiple manufacturing processes—defined as the vertical and horizontal integration of models. We define *vertical integration* as the integration of models and simulations of different phenomenon that occur at multiple length scales for a specific manufacturing process so as to generate information that can be passed to other manufacturing processes that follow. We define *horizontal integration* as the integration of different such manufacturing processes using simulation models ensuring proper flow of the information generated through vertical integration at each manufacturing process thereby establishing the processing-structure-property-performance route to realize an end product [17,18]. To achieve vertical and horizontal integration of models, there must be analysis models linking different manufacturing processes and phenomena, which predict the material properties associated with these processes and ensure the proper forward flow of information. Once we achieve forward modeling, we carry out top-down (goal-oriented), decision-based design exploration of the material microstructure and processing paths to achieve the required product properties. The primary mathematical construct used in the method is the compromise decision support problem (cDSP) supported by the concept exploration framework (CEF) to generate *satisficing* design solutions [19]. Our intention in solving the compromise DSP is to *satisfice* a set of goals and thus we approach the problem from the school of thought of a *satisficer*; more information available in Ref. [20]. The concept exploration framework is inspired from the robust concept exploration method proposed by Chen et al. [21] to systematically generate satisficing, top-level specifications.

In Sec. 2, we describe the vertical and horizontal integration of models from the perspective of the steel manufacturing process chain problem focused on hot rod rolling (HRR) process that we are addressing. In Sec. 3, we describe the CEF and the cDSP construct. In Sec. 4, the proposed goal-oriented, inverse method is described. The empirical models and the response surface models for computational analysis of the problem are presented in Sec. 5. The mathematical formulation of the hot rod rolling process chain is provided in Sec. 6 and the ternary analysis for visualizing and exploring the solution space is covered in Sec. 7 with closing remarks in Sec. 8.

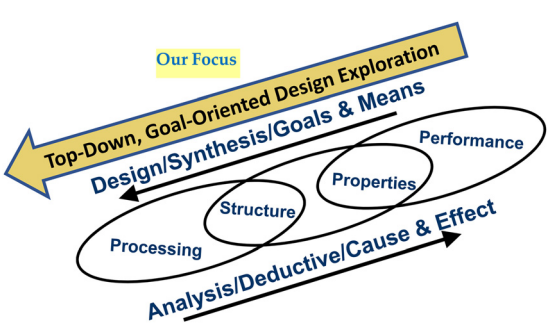

Fig. 1 Olson's hierarchical concept of materials-by-design [3]

2 Integrated Design of Materials, Products and Processes—the Steel Manufacturing Process Chain Problem

Many algorithms for establishing forward relationships have been developed. These models are used to predict the behavior of materials during complex manufacturing processes as the final properties of the end steel product depend on its processing route [22–27]. It is beneficial for steel manufactures to develop computer algorithms/tools that provide the capability to establish inverse relationships; i.e., relate the end properties of the steel product as a function of process variables. These computer algorithms/tools need to be developed using mathematical models that predict the microstructure and mechanical properties of the material as a function of the manufacturing process conditions. The challenge here is in considering all the different phenomena that happen during the processing of the material and establishing the processing-structure-property-performance relationship in an inverse manner using models. In this problem, we are interested in developing an integrated method that is generic and has the ability to relate the end mechanical properties of the material with good accuracy to the different processing and microstructure routes available for the material. The efficacy of the method is illustrated for the specific steel manufacturing process chain problem addressed below. The industry inspired problem is contributed by Tata Consultancy Services Research and Tata Steel in India; the focus being to integrate the design of steel (material), manufacturing processes and automotive gears (end product) [28].

A difficulty during steel making is the distortion that happens in gear blanks during forging and heat treatment requiring more

machining in the later stages of the manufacturing process. This distortion is mainly due to the banded microstructure that forms due to the presence of segregates. The segregation of alloying elements like manganese (Mn) occurs during casting solidification and this impacts the entire downstream processing affecting the end product mechanical properties. These segregates form due to the limited solubility of alloying elements in the melt during casting. These micro segregation patterns usually remain in the material at the later stages as complete removal of these patterns through processes like reheating is not feasible from a manufacturing stand point as it demands large reheating time leading to increased manufacturing costs. In the hot rolling process, deformation of these structures takes place resulting in a change in the concentration profile. The regions are flattened with alternate layers of high solute and low solute develops during rolling. During the following cooling process, phase transformation occurs and austenite to ferrite phase transformation occurs.

If the steel has hypo eutectoid composition, the ferrite phase forms in regions with low austenite stabilizing solute and the remainder transforms to pearlite. Due to the alternate layers of low and high solute regions induced during hot rolling, a banded microstructure having ferrite and pearlite forms with that finally leading to distortion in gear blanks. To manage the effects of distortion at the end of forging, these segregates must be tracked in the previous manufacturing stages and the factors must be managed effectively. These factors could be the operating set points needed for rolling and cooling to produce a specific microstructure. Managing these factors will affect the final mechanical properties of the product. Thus, to predict the mechanical properties of the product as a function of the composition, rolling and cooling factors, there must be an integration of models. The vertical integration of models at multiple length scales and horizontal integration of different processes ensures proper flow of information across processing-microstructure-final mechanical property/performance spaces, see Fig. 2.

The forward modeling starts with the vertical integration of the hot rolling process, which includes a hot deformation module, recrystallization module, flow stress module, and a grain growth module. The input is the chemical composition, initial austenite grain size (AGS) after reheating, and the rolling schedule (strain, strain rate, interpass time, number of passes). These are used to predict the temperature evolution, flow stress, and to estimate the austenite grain size after rolling. The output after the vertical integration of these modules is passed to cooling process models. In the vertical integration of cooling process, time–temperature transformations and simultaneous transformations must be considered for the transformations from austenite to different steel phases. This will provide a way to model the banding that occurs during cooling. Here, we consider austenite transformations to ferrite and pearlite phases only. The input to this module is the chemical composition, final austenite grain size after rolling, and the cooling conditions (cooling rate). After the vertical integration of these modules, the output is the phase fractions (final microstructure after cooling), pearlite interlamellar spacing and the ferrite

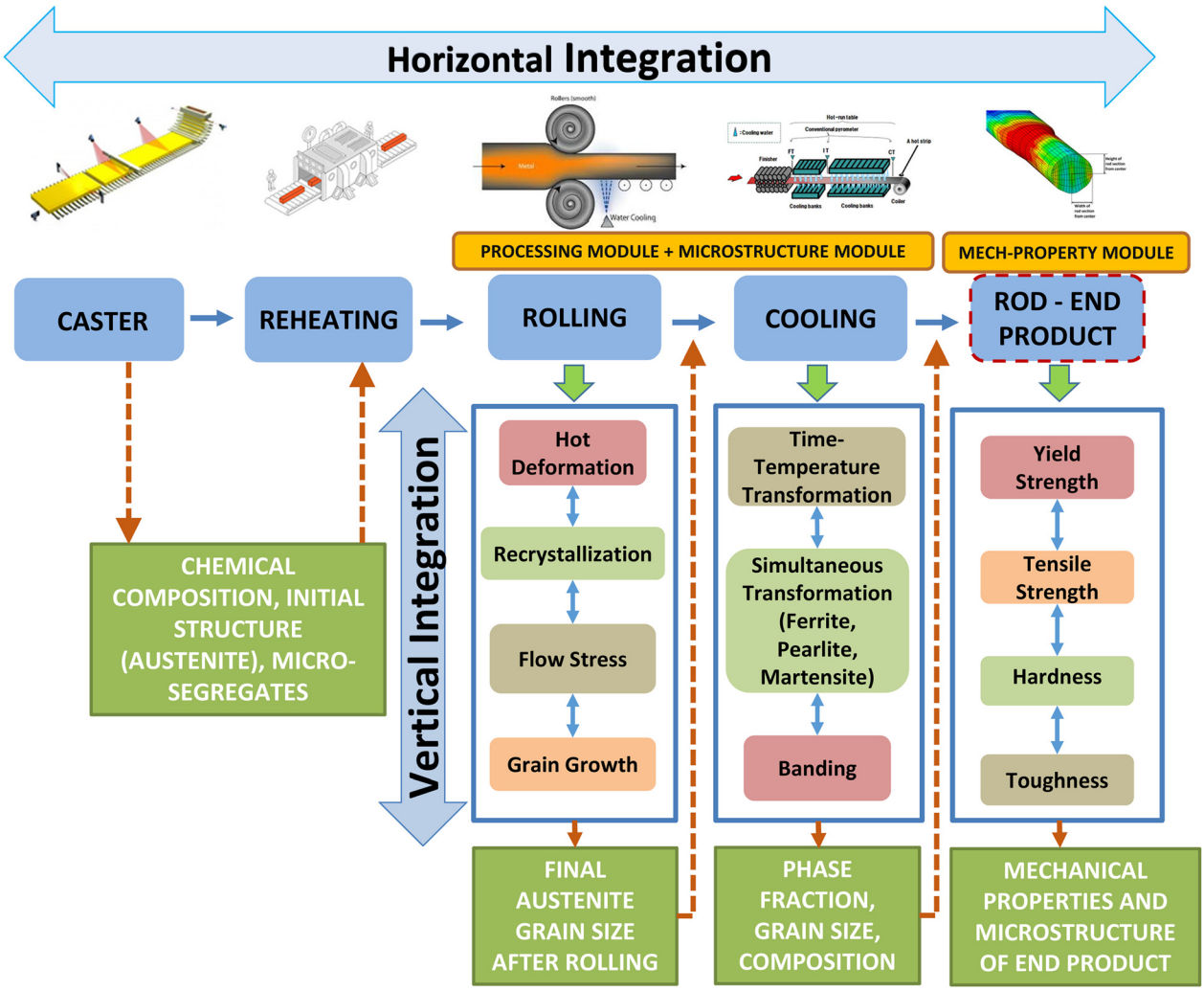

Fig. 2 The vertical and horizontal integration of models with information flow for the hot rod rolling process chain

grain size. This output and the chemical composition serve as the input for the property module to predict the mechanical properties, the yield strength, tensile strength, hardness, and toughness. Through these model and simulation integrations, specific problem-dependent information is passed from one manufacturing process to the other thereby developing a link between the manufacturing processes. This is the horizontal integration of the manufacturing processes to realize the end product (rod produced after rolling and cooling for this problem) by establishing the process-structure-property-performance relationships. To illustrate the goal-oriented inverse method, we define a boundary within the problem. Here, we focus on using the proposed method to establish processing-microstructure-property relations between the rolling, cooling module (processing and microstructure) and the property module of the product that defines the end performance. In Sec. 3, the concept exploration framework that is used to systematically formulate the problem and identify ranged set of satisficing solutions is described.

3 The Concept Exploration Framework

The CEF is introduced in this paper as a general framework that includes systematic steps to identify design alternatives and generate *satisficing* design solutions. The CEF is inspired from the robust concept exploration method [21] with addition of features (processors) to consider different material and product models and options to explore the solution space for different design scenarios. Core to the CEF is the foundational mathematical construct—the cDSP [19]. The cDSP construct used here is anchored in the robust design paradigm first proposed by Taguchi. The fundamental assumption is that the models are not complete, accurate, and of equal fidelity [29,30]. The cDSP is a hybrid of mathematical programming and goal programming. Target values for each goal are defined in a cDSP and the emphasis of the designer is to satisfy these target goals as closely as possible. This is achieved by seeking multiple solutions through trade-offs among multiple conflicting goals. The solutions obtained are further evaluated by solution space exploration to identify solution regions that best satisfy the requirements identified. There are four keywords in the cDSP—*Given*, *Find*, *Satisfy,* and *Minimize*. The overall goal of the designer using the cDSP is to minimize a deviation function—a function formulated using the deviations (captured using *deviation variables*) that exists from the goal targets. The details regarding formulating and solving the cDSP are available [19,30] and are not explained here.

Next, we explain the CEF. In Fig. 3, the computing infrastructure for the CEF is shown. The computing infrastructure for CEF includes eight processors (A, B1, B2, D, E, F, G, H) and

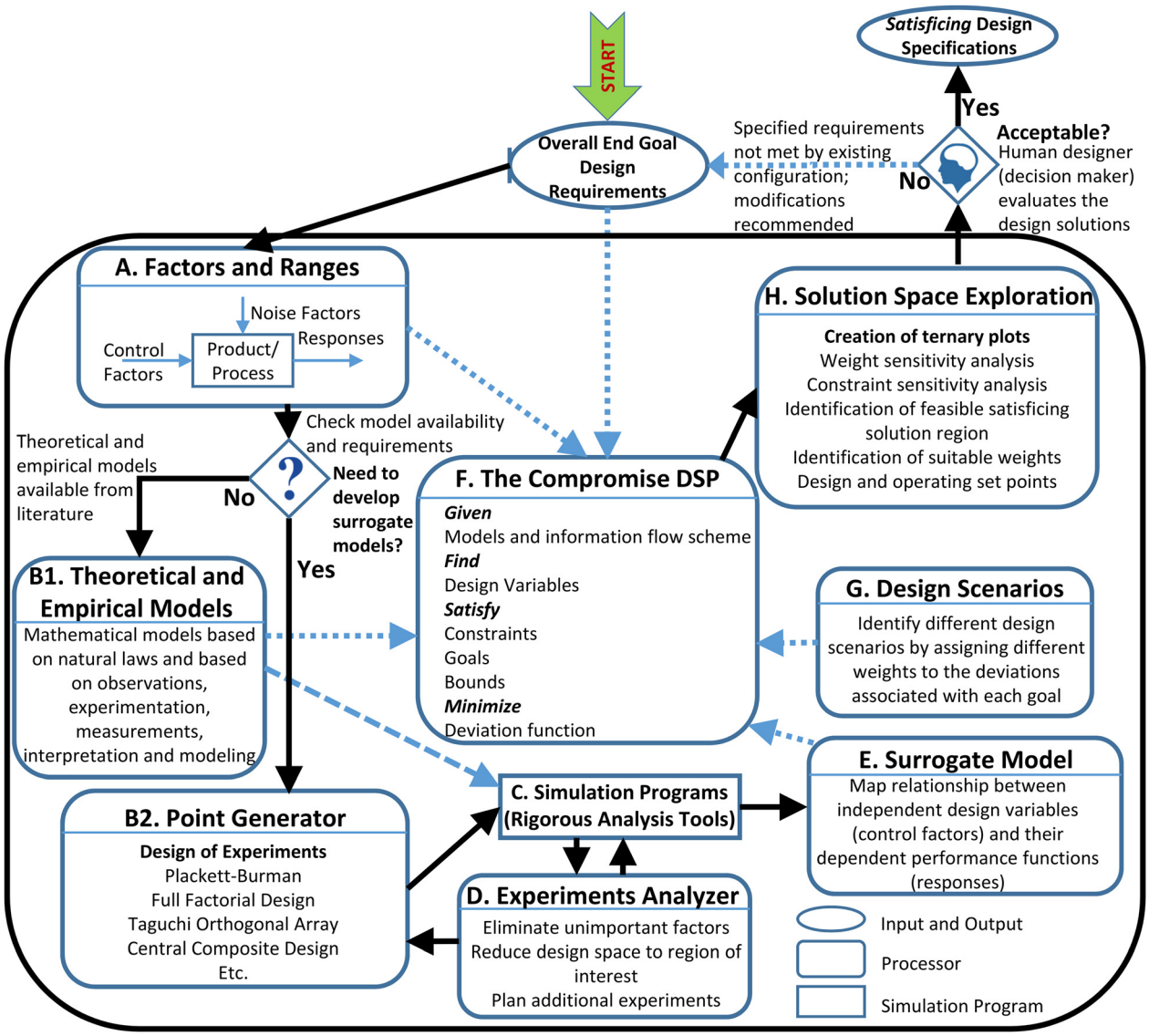

Fig. 3 The computing infrastructure for CEF

simulation programs (C). The application of the CEF begins with the designer identifying the overall end goal design requirements for the problem under study. The further steps in the CEF are below. The solid arrows in Fig. 3 are used to highlight the steps of CEF in sequence. The dotted lines and dashed lines are used to represent information sharing within the framework.

3.1 Step 1 Using Processors A and B1. In this step, the initial concept exploration space is defined and the cDSP is formulated. For the requirements identified for the problem, the control factors (factors that the designer can control), noise factors (factors that the designer cannot control), and the responses (the performance goals identified) and their ranges are identified in processor A. This information is input to the foundational mathematical construct—the cDSP, processor F. In parallel with the identification of factors, ranges, and responses, a designer identifies the models available/required. For problems related to manufacturing processes such as hot rolling and cooling, several different models defining material/process behavior are available in the literature [22–25,31]. Such available theoretical and empirical models are identified in processor B1 and are communicated to the cDSP.

3.2 Step 2 Using Processors B2, D, E and Simulation Program C. In step 2, the designer carries out low-order screening experiments. If models for the problem are not available or if there is a need to develop reduced order or surrogate models so as to reduce the size of the problem, an experiment is designed to develop them. The point generator, processor B2, is used to design the experiments. The simulation program (C) is used to run the experiments. The simulation programs for manufacturing related problems may use some of the theoretical and empirical models from processor B1. This information flow is shown using the dotted arrow in Fig. 3. An example of this is a finite element simulation (Simulation Program, C) for rolling that uses a constitutive model (empirical model, Processor B1) to define the flow behavior of the material. The experiments analyzer, processor D, evaluates the simulation results and recommends additional experiments if needed. Regression analysis and ANOVA are used to evaluate the significance of the results. Processor E is used to create the surrogate models using the simulation program results that are acceptable to the designer.

3.3 Step 3 Using Processors F, G and H. All models are communicated to the cDSP, processor F. The cDSP is then exercised for different design scenarios as specified by processor G. These scenarios, which are identified by assigning different weights to the deviations associated with the goals, define a solution space. This solution space is then explored using processor H. Ternary plots are generated to visualize and explore the solution space to identify feasible solution regions that satisfy the requirements. A human designer evaluates the design solutions, checks feasibility and satisficing solution regions. If the overall end goal requirements are not satisfied or there are no feasible satisficing regions, the overall end goal requirements may be modified as in Fig. 3. In such a situation, a designer can also make use of the ternary plots to carry out design trade-offs to identify regions that satisfy the modified end goal requirements instead of repeating the CEF.

Thus, the generic functionalities offered by CEF in summary include: (i) identification of end goals and requirements for a problem, (ii) systematic identification of control factors, noise factors that influence the responses of the goals and requirements, (iii) systematic identification of mathematical models—theoretical, empirical models available from literature on the problem domain and systematic development of surrogate models using simulation programs and design of experiments, (iv) systematic formulation of the design problem using the cDSP construct for the given information available for the problem, (v) systematic planning of the design scenarios to be explored for the problem, (vi) exercising the problem formulated for the design scenarios, and (vii) systematic analyzing of the solution space with the opportunity for the human designer to visualize the solution space and make design decisions. These functionalities can be used to formulate and execute any complex systems problem in a systematic fashion to provide decision support provided availability of required information. To facilitate the generic applicability of the CEF and extend the designer's abilities in making design decisions that are robust, flexible, and modifiable particularly in the early stages of design, an ontology for design space exploration and a template-based ontological method that supports systematic design space exploration using CEF is proposed in our recent paper [32].

The concept of exploration framework along with its features of multigoal decision support can be readily incorporated into a design method that supports the design of the material and product (processing, composition, and microstructure) as part of a larger overall systems design process. The framework can embody the hierarchy of process-structure-property-performance proposed by Olson [3] by systematically accounting the information flow and mappings across these spaces and transforming overall design requirements into a set of satisficing design specifications for the material-product-and manufacturing process system of interest.

In Sec. 4, we describe the goal-oriented, inverse method in its generic form and the application of the method to explore the design space for the hot rod rolling process chain problem.

4 The Goal-Oriented, Inverse Method

4.1 Generic Form of the Goal-Oriented, Inverse Method. The basic idea of our method for finding satisficing solutions in a multilevel, multistage process chain that involves the PSPP relations is passing down the satisficing solution ranges in an inverse manner, from given final performance range to the design space of the previous space (defined by model input and output) with designer having the flexibility to choose solution of preference. The method will be explained using the information flow diagram shown in Fig. 4. It is a *goal-oriented* method because we start with the end goals that need to be realized for the product as well as process and then design the preceding stages to satisfy these end goals as closely as possible by exploring the design space. Then the design decisions that are made for the end requirements of the product/process after exploration are communicated to the stages that precede them to make logical decisions at those stages to satisfy the requirements identified thereby carrying out a design space exploration process in an inverse manner, as described by steps 2.1–2.3, Fig. 4. To demonstrate the generic nature of the method, we call the different sequential processes as "n" to "$n+2$" and the decision support constructs as 'i' to '$i+2$'.

4.1.1 Step 1: Establish Forward Modeling and Information Flow Across the Process Chain (Forward Material Workflow). Step 1 of the proposed method involves establishing the forward modeling and information flow across models. In step 1, the designer makes sure that there is proper flow of information as models are connected across different "Processes." These processes could be different manufacturing processes that are sequentially connected to produce the product with information passing across processing-microstructure-property-performance spaces. Mathematical models are either identified or developed to establish the information flow. The steps 1 and 2 of the concept exploration framework are used to identify factors, ranges, responses, and models for the specific materials design problem under study. In Fig. 4, step 1, we see that the output of a process serves as the input for the next process along with other new inputs specific to the next process with the final output being the end product. We can imagine these "processes n, $n+1$ and $n+2$" as processing, microstructure, and property spaces respectively as shown in Fig. 4 to understand the method clearly. Thus, process n (processing space) generates output that serves as input for process $n+1$ (the microstructure space). The output of process $n+1$ (the

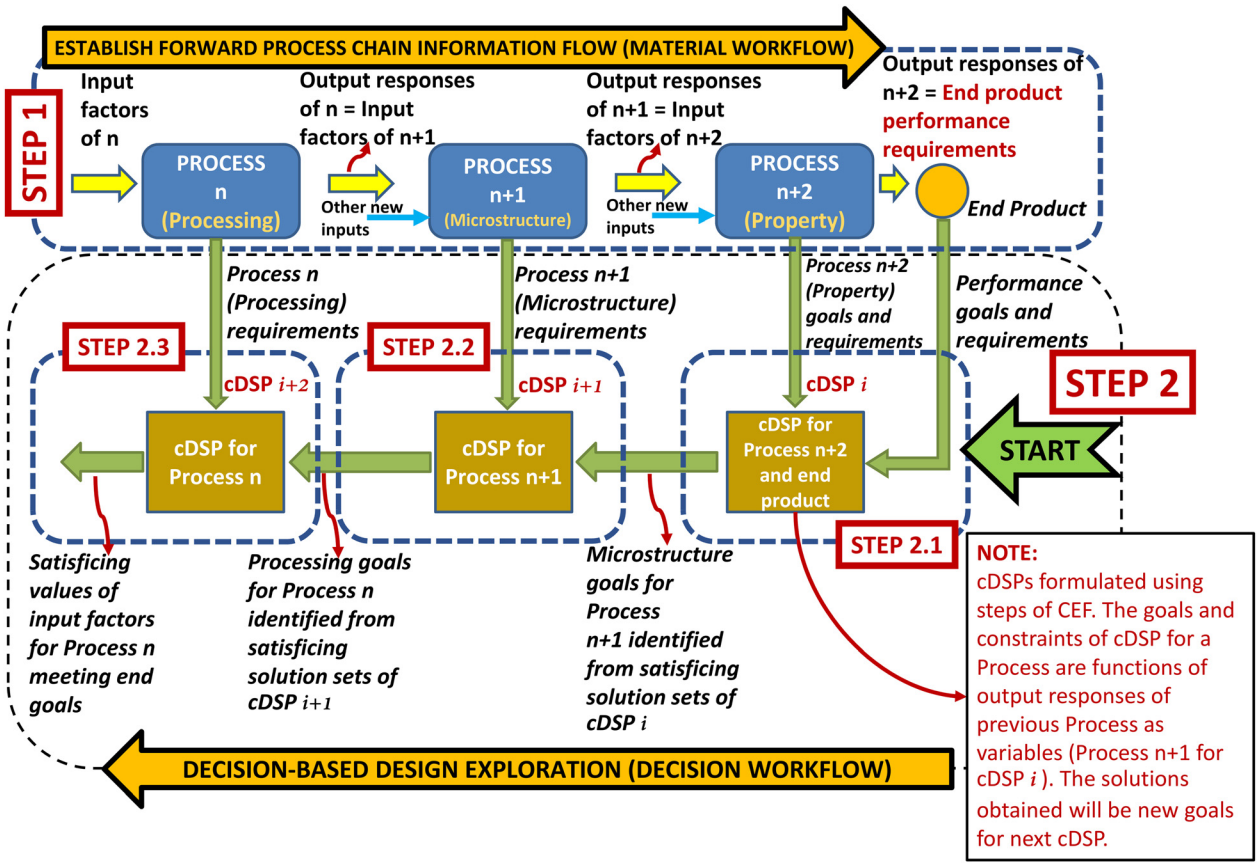

Fig. 4 Generic form of the goal-oriented, inverse method illustrated using steps 1 and 2

microstructure identified) serves as the input for process $n+2$. The output of process $n+2$ defines the property space and this directly defines the final performance characteristics of the end product. From a design standpoint, the inputs to a process are design variables and the output response from the process serves as input variables to next process.

4.1.2 Step 2: Carry out Decision-Based Design Exploration Starting From Performance Space and Sequentially Identifying Satisficing Regions of Interest in Previous Spaces in an Inverse Manner

4.1.2.1 Step 2.1: Formulate compromise decision support problem i using concept exploration framework for achieving the desired end product properties and performances. In step 2, we begin the decision-based design exploration starting from the end goals and requirements that are identified. The exploration of the process chain shown in Fig. 4 is completed using steps 2.1–2.3. cDSP i is formulated for process $n+2$ in step 2.1. The design variables of this cDSP will be the output responses from process $n+1$ that serves as input to process $n+2$. The property and performance goals that are desired are defined in this cDSP. On executing the cDSP for different design scenarios and exploring the solution space using CEF, the designer is able to identify the combination of output responses from process $n+1$ (that serves as input for process $n+2$) that best satisfy the conflicting property and performance goals defined. The identified values of output responses for process $n+1$ that satisfies the goals defined for cDSP i are passed as goals for cDSP $i+1$. In Fig. 4, process $n+1$ represents the microstructure space; then the output of cDSP i will be the target values of microstructure factors that satisfies the properties and performances defined for the product. In step 2.2, using cDSP $i+1$, we analyze how these target microstructure values can be achieved in Process $n+1$ with the output responses from Process n as the input variables.

4.1.2.2 Step 2.2: Formulate compromise Decision Support problem i+1 using concept exploration framework for achieving the goals identified for Process n+1 based on the exploration carried out in compromise decision support problem i. In step 2.2, we formulate cDSP $i+1$ for Process $n+1$. The target goals in this cDSP are the values of the design variables for cDSP i identified after solution space exploration in step 2.1. The design variables for cDSP $i+1$ are the output responses from process n that serves as input to process $n+1$. Executing this cDSP and exploring the solution space using CEF, the designer is able to identify the combination of input variables that best satisfies the target goals defined. From Fig. 4, we see that the output will the combination of processing variables that best satisfy the microstructure targets defined in cDSP $i+1$. Again, we pass these identified values of design variables from cDSP $i+1$ that satisfy requirements to next cDSP $i+2$ as target goals.

4.1.2.3 Step 2.3: Formulate compromise decision support problem i+2 using concept exploration framework for achieving the goals identified for Process n based on the exploration carried out in compromise decision support problem i+1. In step 2.3, in a similar fashion to previous steps, the designer formulates cDSP $i+2$ for process n with target goals being the design variable values identified from cDSP $i+1$. On exploration of solution space, the designer is able to identify the combination of input factors of process n that best satisfies the targets performance goals identified for cDSP $i+2$.

Thus, using this proposed method, the designer is able to carry out top-down driven, simulation-supported, decision-based design of processing paths and material microstructure to satisfy a ranged set of product-level performance requirements. The method is generic and can be applied to similar problems with information flow from one process to another as shown in Fig. 4. The method supports coordination of information and human decision-making

and is suited for problems involving a network of forward, sequential information flow. Given any complex system that involves sequential flow of information across processes/levels, the proposed method has the potential to be applied to support information flow by making effective decisions across the processes/levels in order to realize an end goal.

4.2 Application for the Hot Rod Rolling Process Chain Problem. In Fig. 5, we show the schematic application of proposed goal-oriented, inverse method to carry out the integrated design exploration of the hot rod rolling process chain problem of interest.

4.2.1 Step 1: Establish Forward Modeling and Information Flow Across the Process Chain. For the hot rod rolling process chain problem addressed in this paper, the mechanical property goals and requirements for yield strength (YS), tensile strength (TS), hardness (HV), and toughness measured by impact transition temperature (ITT). These mechanical properties are dependent on the final microstructure after cooling like the ferrite grain size after cooling (FGS, D_α), the phase fractions of ferrite (X_f) and pearlite ($1 - X_f$), the pearlite interlamellar spacing (S_0) and the composition variables like silicon [Si], nitrogen [N], phosphorous [P] and manganese [Mn]. These microstructure factors are defined by the rate (CR) at which cooling is carried out and the final austenite grain size after rolling (AGS, D) and composition variables like carbon [C] and manganese [Mn]. The AGS is determined by the processing carried out at rolling stage, which requires the modeling of hot deformation, recrystallization, grain growth, etc. The input to the cooling stage is D, CR, [C] and [Mn] from the rolling process. The outputs are D_α, X_f, and S_0, which, along with the composition variables, define the YS, TS, ITT, and HV of end rod produced. The models used to establish these relationships are presented in Sec. 5.

4.2.1.1 Step 2.1: Formulate compromise decision support problem for end mechanical properties of rod to explore the processing and microstructure space for cooling stage. In step 2.1, the cDSP for the mechanical properties of the final end product is formulated. Information, requirements, and the correlations between mechanical properties and microstructure after cooling (ferrite grain size, pearlite interlamellar spacing, phase fractions, and composition) are communicated to this cDSP. The end mechanical property goals are requirements for yield strength, tensile strength, hardness and toughness (impact transition temperature). On exercising the cDSP and carrying out solution space exploration of the microstructure space after cooling, the combinations for ferrite grain size (D_α), phase fractions X_f, pearlite interlamellar spacing S_0, and compositions that best satisfy the requirements for end properties are identified and are communicated to the next step. The formulation of the cDSP is provided in Sec. 6 and the solution space exploration is carried out in Sec. 7.

4.2.1.2 Step 2.2: Formulate compromise decision support problem for cooling stage to explore the processing and microstructure space of rolling. In step 2.2, a similar process to that in step 2.1 is carried out to formulate the cDSP for cooling. This cDSP has target goals and requirements for ferrite grain size D_α, phase fraction X_f, and composition that are based on the solutions obtained from the first cDSP. Also, information from cooling stage such as banding requirements and cooling rate requirements are included into this cDSP. The information, requirements, and correlations of variables at the end of rolling (austenite grain size,

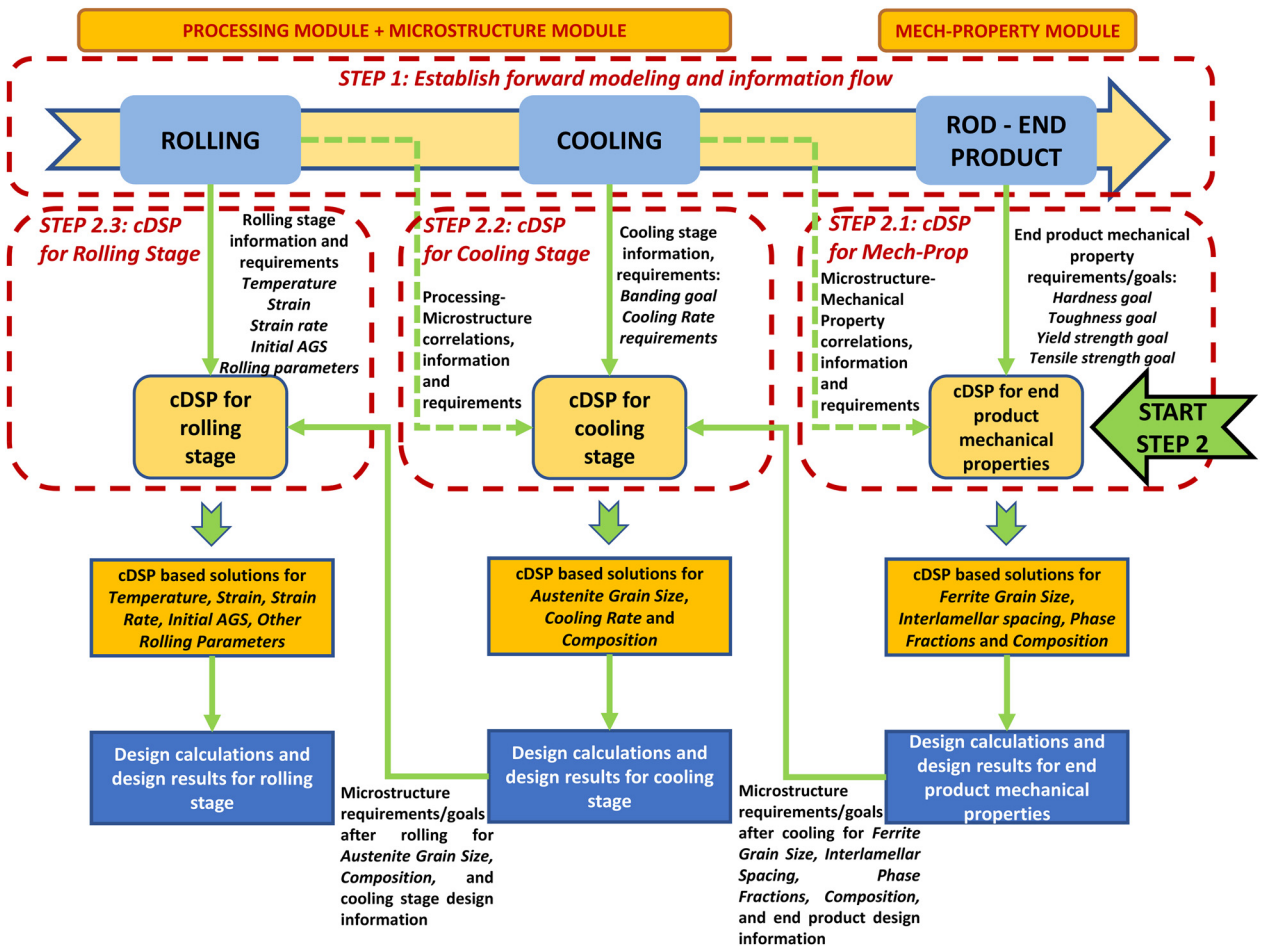

Fig. 5 Schematic of the proposed goal-oriented, inverse method for the hot rod rolling process chain problem

Table 1 Mechanical property models

Mechanical Property	Model	Reference
Yield Strength	$YS = X_f\left(77.7 + 59.9 \times [\text{Mn}] + 9.1\times(0.001D_\alpha)^{-0.5}\right) + 478[\text{N}]^{0.5} + 1200[\text{P}] + (1 - X_f)[145.5 + 3.5S_0^{-0.5}]$ (1) where YS is in MPa, S_o in μm, D_α in μm	Kuziak and co-authors [23]
Tensile Strength	$TS = X_f\left(20 + 2440 \times [\text{N}]^{0.5} + 18.5 \times (0.001D_\alpha)^{-0.5}\right) + 750(1 - X_f) + 3\left(1 - X_f^{0.5}\right)S_0^{-0.5} + 92.5 \times [\text{Si}]$ (2) where TS is in MPa, S_o in μm, D_α in μm	Kuziak and co-authors [23]
Hardness	$HV = X_f\left(361 - 0.357T_{mf} + 50[\text{Si}]\right) + 175(1 - X_f)$ (3) Average austenite to ferrite transformation temperature (T_{mf}) is assumed as 700° C	Yada [35]
Impact Transition Temperature	$ITT = X_f\left(-46 - 11.5D_\alpha^{-0.5}\right) + (1 - X_f) \times \left(-335 + 5.6S_0^{-0.5} - 13.3p^{-0.5} + (3.48 \times 10^6)t\right) + 49[\text{Si}] + 762[\text{N}]^{0.5}$ (4) where D_α, S_o, p and t are in mm. We have assumed the value of pearlite colony size p as 6 μm and carbide thickness t as 0.025 μm	Gladman and co-authors [34]

composition) and the cooling stage parameters are communicated to the cDSP. The goals for this cDSP are target ferrite grain size and target phase fractions subject to constraints. On exercising the cDSP, the combinations for austenite grain size D, cooling rate CR, and composition elements like carbon (C) and manganese (Mn) that best satisfy the requirements are identified. The formulation of this cDSP is in Sec. 6 and the solution space exploration is carried out in Sec. 7.

4.2.1.3 Step 2.3: Formulate compromise decision support problem for rolling to carry out design exploration of rolling process variables. In step 2.3, we follow a similar procedure to steps 2.1 and 2.2 to formulate the cDSP for rolling considering the information generated from cooling and the rolling information and requirements identified. This cDSP has a grain growth module, static, dynamic, and meta dynamic recrystallization modules and a hot deformation module.

Due to the complexity and size of the problem, we are demonstrating the efficacy of method by carrying out the design space exploration of the hot rolling process chain problem by addressing the cDSPs in steps 2.1 and 2.2. The cDSPs in steps 2.1 and 2.2 span the processing, microstructure, and property spaces and are thus sufficient for framing a well-defined problem boundary for the method demonstration.

5 Mathematical Models for Hot Rod Rolling Process Chain Design (Establishing Step 1 of Method)

The mathematical models used to formulate the HRR process chain problem are introduced and brief descriptions are provided here. These models, the control variables, noise factors, parameters, responses, and allowable ranges are identified by carrying out steps 1 and 2 of the CEF as described in Sec. 3. From the problem perspective, we accomplish step 1 of the goal-oriented, inverse decision-based design method by identifying these forward models to establish the relationships described in Sec. 4. In Sec. 5.1, we describe the microstructure-mechanical property correlation models that establish relationships between the mechanical properties of the rod product and the microstructure generated after cooling stage. In secs. 5.2 and 5.3, we describe the models for phase transformation on cooling after hot rolling.

5.1 Mechanical Property–Microstructure Correlation Models. The required mechanical properties for the rod are yield strength (YS), tensile strength (TS), toughness measured by ITT and hardness (HV). Gladman et al. [33,34] predict the mechanical properties of plain carbon steel products as a function of the ferrite-pearlite microstructure. Models with improved predictive power were later developed by Hodgson and Gibbs [22], Majta et al. [24], Kuziak et al. [23] and Yada [35], Table 1. Details on these models and the reason for their selection are presented by Nellippallil et al. [36].

5.2 Models for Phase Transformation on Cooling After Hot Working. Classical nucleation and grain growth theory quantitatively describe the kinetics of decomposition of austenite. Using classical Johnson-Mehl-Avrami theory, we describe the transformation of a single phase to a product phase [27]. The transformations that occur in steel are often simultaneous resulting in the formation of multiple phases such as allotriomorphic ferrite, Widmanstätten ferrite, bainite, pearlite, and martensite. Therefore, one requirement for a kinetic model for the phase transformation of steel is that it must allow for simultaneous phase transformations resulting in different steel phases. Robson and Badeshia [37] and Jones and Badeshia [38] address this requirement by numerically solving all impingement equations and choosing the appropriate nucleation and grain growth equations. The simultaneous transformation of austenite into allotriomorphic ferrite, Widmanstätten ferrite, and pearlite is considered by Jones and

Table 2 Factors and factor levels for DoE

Level	*CR* K/min	*AGS* μm	[C] %	[Mn] %
1	11	30	0.18	0.7
2	55	55	0.24	1.1
3	100	100	0.3	1.5

Table 3 RSM for phase fractions

Phase fraction	Response surface model developed	R^2 value
Allotriomorphic ferrite	$X_{fa} = 1.59 - 0.26[C] - 0.00856CR - 0.0105D - 3.08[C] + 0.000826[Mn]CR + 0.0009[Mn]D + 0.7647[Mn][C] + 0.000011CR*D + 0.002CR[C] + 0.0032D[C] - 0.05058[Mn]^2 + 0.00004CR^2 + 0.000036D^2 + 2.483[C]^2$ (5)	0.98
Pearlite	$X_p = 0.206 - 0.117[Mn] - 0.0005CR - 0.00113D + 0.248[C] + 0.00032[Mn]CR + 0.000086[Mn]D + 0.9539[Mn][C] - 4.259 \times 10^{-6}CR*D + 0.00726CR[C] + 0.0023D[C] - 0.0305[Mn]^2 - 0.0000056CR^2 + 4.859 \times 10^{-6}D^2 + 0.79[C]^2$ (6)	0.99
Widmanstätten Ferrite	$X_{fw} = 1 - (X_{fa} + X_p)$ (7)	—
Total ferrite	$X_f = (X_{fa} + X_{fw})$ (8)	—

Badeshia [38]; details can be found in Refs. [27,38], and [39]. We have used the program STRUCTURE developed by Jones and Badeshia to predict the simultaneous transformation of austenite [40].

Response surface models (RSMs) are used to calculate the microstructure (allotriomorphic ferrite, Widmanstätten ferrite, and pearlite) of steel as a function of percentages of carbon [C] manganese [Mn], cooling rate *CR*, and austenite grain size [D] using the STRUCTURE program. These predictors are selected because of their substantial contribution to austenite transformation and the formation of banded microstructure [27]. Values for the other required input are based on the work of Jones and Badeshia [38]. A fractional factorial design of experiments is carried out to develop response surface models for the transformation of austenite to ferrite and pearlite [23,25], Table 2. The response surface models are shown in Table 3. The RSMs are verified by comparing the predictions with experimental (measured) data reported by Bodnar and Hensen [41], see Nellippallil et al. [36].

5.3 Models for Ferrite Grain Size (D_α) and Pearlite Interlamellar Spacing (S_o). As the hot worked steel cools, austenite is transformed into various phases. The most important parameters are the ferrite grain size and pearlite interlamellar spacing because they contribute to the steel's mechanical properties. The models for these parameters are shown in Table 4.

6 Formulation of the Cdsps for Hot Rolling Process Chain Problem

In step 2.1 of the method, we formulate the cDSP for the desired end mechanical properties of the product, Table 5. We then determine the end mechanical properties as a function of microstructure factors (D_α, X_f, S_0, Mn, Si, N) after cooling. The end mechanical property goals, e.g., maximizing YS, TS, and HV, are captured in the cDSP. The requirement for minimizing impact transition temperature is captured as a constraint. The possible achievement of these conflicting goals is characterized by solution space exploration. The upper and lower limits for the system variables and the maximum and minimum values for the mechanical properties are defined in the cDSP as bounds and constraints. The goal targets are $YS_{Target} = 330$ MPa, $TS_{Target} = 750$ MPa, $HV_{Target} = 170$. The requirement for ITT is to achieve the minimum value. The requirement for managing the banded microstructure is considered during solution space exploration.

Table 4 Models for D_α and S_o

Parameter	Model	Reference
Ferrite grain size	$D_\alpha = \left(1 - 0.45\varepsilon_r^{0.5}\right) \times \left\{(-0.4 + 6.37C_{eq}) + (24.2 - 59C_{eq})CR^{-0.5} + 22\left[1 - \exp(-0.015D)\right]\right\}$ (9) for $C_{eq} < 0.35$ $D_\alpha = \left(1 - 0.45\varepsilon_r^{0.5}\right) \times \{(22.6 - 57C_{eq}) + 3CR^{-0.5} + 22\left[1 - \exp(-0.015D)\right]$ for $C_{eq} > 0.35$ (10) where D is the final AGS after rolling and ε_r is retained strain. C_{eq} is the carbon equivalent given by Eq. (11). $C_{eq} = (C + Mn)/6$ (11)	Hodgson and Gibbs [22]
Pearlite interlamellar spacing	$S_o = 0.1307 + 1.027[C] - 1.993[C]^2 - 0.1108[Mn] + 0.0305CR^{-0.52}$ (12)	Kuziak and co-authors [23]

Table 5 The cDSP formulation for Step 2.1

Given

(1) End requirements identified for the rod rolling process
- Maximize Yield Strength (Goal)
- Maximize Tensile Strength (Goal)
- Maximize Hardness (Goal)
- Minimize ITT (Requirement)
- Manage Banded Microstructure (Requirement)

(2) Well established empirical and theoretical correlations, RSMs and information flow from the end of cooling to the end product mechanical properties (Details provided in Sec. 5)

(3) System variables and their ranges

Find

System Variables

X_1, ferritegrainsize(D_α)
X_2, the phase fraction of ferrite (X_f)
X_3, the pearlite interlamellar spacing (S_0)
X_4, manganese concentration after cooling ([Mn])
X_5, the composition of Si ([Si])
X_6, the composition of N ([N])

Deviation Variables

$d_i^-, d_i^+, i = 1,2,3$

Satisfy

System Constraints

- Minimum yield strength constraint

$$\mathrm{YS} \geq 220 \text{ MPa} \tag{13}$$

- Maximum yield strength constraint

$$\mathrm{YS} \leq 330 \text{ MPa} \tag{14}$$

- Minimum tensile strength constraint

$$\mathrm{TS} \geq 450 \text{ MPa} \tag{15}$$

- Maximum tensile strength constraint

$$\mathrm{TS} \leq 750 \text{ MPa} \tag{16}$$

- Minimum hardness constraint

$$\mathrm{HV} \geq 131 \tag{17}$$

- Maximum hardness constraint

$$\mathrm{HV} \leq 170 \tag{18}$$

- Minimum ITT constraint

$$\mathrm{ITT} \geq -100\,^\circ\mathrm{C} \tag{19}$$

Maximum ITT constraint

$$\mathrm{ITT} \leq 100\,^\circ\mathrm{C} \tag{20}$$

System Goals

Goal 1:
- Maximize Yield Strength

$$\frac{\mathrm{YS}(X_i)}{\mathrm{YS}_{\mathrm{Target}}} + d_1^- - d_1^+ = 1 \tag{21}$$

Goal 2:
- Maximize Tensile Strength

$$\frac{\mathrm{TS}(X_i)}{\mathrm{TS}_{\mathrm{Target}}} + d_2^- - d_2^+ = 1 \tag{22}$$

Goal 3:
- Maximize Hardness

$$\frac{\mathrm{HV}(X_i)}{\mathrm{HV}_{\mathrm{Target}}} + d_3^- - d_3^+ = 1 \tag{23}$$

Variable Bounds

$8 \leq X_1 \leq 25(\mu\text{m})$

$0.1 \leq X_2 \leq 0.9$

$0.15 \leq X_3 \leq 0.25(\mu\text{m})$

$0.7 \leq X_4 \leq 1.5(\%)$

$0.18 \leq X_5 \leq 0.3(\%)$

$0.007 \leq X_6 \leq 0.009(\%)$

Bounds on deviation variables

$$d_i^-, d_i^+ \geq 0 \text{ and } d_i^- * d_i^+ = 0, \text{i} = 1, 2, 3 \tag{24}$$

Minimize

We minimize the deviation function

$$Z = \sum_{i=1}^{3} W_i \left(d_i^- + d_i^+\right); \quad \sum_{i=1}^{3} W_i = 1 \tag{25}$$

On exercising the cDSP and carrying out solution space exploration, a process designer is able to solve and capture the knowledge associated with the following inverse problem: *Given the end mechanical properties of a new steel product mix, what should be the microstructure factors after the cooling stage that satisfies the requirements?*

On exercising the cDSP for different design scenarios and carrying out solution space exploration, following the steps in concept exploration framework, we obtain the combinations for D_α, X_f, S_0, Mn, Si, N that satisfy the end mechanical properties and other requirements. The desired solutions identified for D_α, X_f, S_0 are then used as the target goals for the next cDSP (step 2.2 of the goal-oriented, inverse method).

In step 2.2 of the method, we formulate the cDSP for the cooling stage, Table 6. Using this cDSP, we relate the microstructure factors after cooling that best satisfy the first cDSP requirements as a function of the microstructure and composition factors (D, C, Mn) after the rolling and the cooling stage operating factor (*CR*). The target values for the goals are defined as $\text{D}_{\alpha\text{Target}}$, $X_{f\,\text{Target}}$, $S_{0\text{Target}}$ as the results from the first cDSP. On exercising

Table 6 The cDSP formulation for step 2.2

Given

(1) Target values for microstructure after cooling (the combination identified from the first cDSP as best satisfying the end goals)
(2) Well established empirical and theoretical correlations, RSMs and complete information flow from the end of rolling to the end product mechanical properties (Details provided in Sec. 5)
(3) System variables and their ranges

Find

System Variables

X_1, Cooling Rate (CR)
X_2, AGS (D)
X_3, the carbon concentration ([C])
X_4, the manganese concentration after rolling ([Mn])

Deviation Variables

$d_i^-, d_i^+, i = 1,2,3$

Satisfy

System Constraints

- Minimum ferrite grain size constraint

$$D_\alpha \geq 8\ \mu\text{m} \tag{26}$$

- Maximum ferrite grain size constraint

$$D_\alpha \leq 20\ \mu\text{m} \tag{27}$$

- Minimum pearlite interlamellar spacing constraint

$$S_o \geq 0.15\ \mu\text{m} \tag{28}$$

- Maximum pearlite interlamellar spacing constraint

$$S_o \leq 0.25\ \mu\text{m} \tag{29}$$

- Minimum ferrite phase fraction constraint (manage banding)

$$X_f \geq 0.5 \tag{30}$$

• Maximum ferrite phase fraction constraint (manage banding)

$$X_f \leq 0.9 \tag{31}$$

• Maximum carbon equivalent constraint

$$C_{\text{eq}} \leq 0.35 \tag{32}$$

Also included are mechanical properties constraints based on the results obtained from first cDSP solution space exploration (the acceptable ranges identified for mechanical properties)

• Minimum yield strength constraint

$$\text{YS} \geq \text{YS}_{\text{lowerlimit}}\ \text{MPa} \tag{33}$$

• Maximum yield strength constraint

$$\text{YS} \leq \text{YS}_{\text{upper limit}}\ \text{MPa} \tag{34}$$

• Minimum tensile strength constraint

$$\text{TS} \geq \text{TS}_{\text{lower limit}}\ \text{MPa} \tag{35}$$

• Maximum tensile strength constraint

$$\text{TS} \leq \text{TS}_{\text{upper limit}}\ \text{MPa} \tag{36}$$

• Minimum hardness constraint

$$HV \geq HV_{\text{lower limit}} \tag{37}$$

• Maximum hardness constraint

$$HV \leq HV_{\text{upper limit}} \tag{38}$$

System goals

The target values for system goals are identified from the solution space exploration carried out for the first cDSP.

Goal 1:

• Achieve ferrite grain size target from cDSP 1

$$\frac{D_{\alpha\text{Target}}}{D_{\alpha}(X_i)} + d_1^+ - d_1^- = 1 \tag{39}$$

Goal 2:

• Achieve Ferrite Fraction from cDSP 1

$$\frac{X_f(X_i)}{X_{f\,\text{Target}}} + d_2^- - d_2^+ = 1 \tag{40}$$

Goal 3:

• Achieve Pearlite Interlamellar Spacing Target from cDSP 1

$$\frac{S_{o\text{Target}}}{S_o(X_i)} + d_3^+ - d_3^- = 1 \tag{41}$$

Variable bounds

$11 \leq X_1 \leq 100(\text{K/min})$
$30 \leq X_2 \leq 100(\mu\text{m})$
$0.18 \leq X_3 \leq 0.3(\%)$
$0.7 \leq X_4 \leq 1.5(\%)$

Bounds on deviation variables

$$d_i^-, d_i^+ \geq 0 \text{ and } d_i^- * d_i^+ = 0, \text{i} = 1, 2, 3 \tag{42}$$

Minimize

We minimize the deviation function

$$Z = \sum_{i=1}^{3} W_i\left(d_i^- + d_i^+\right); \quad \sum_{i=1}^{3} W_i = 1 \tag{43}$$

Table 7 Scenarios with weights for goals

Scenarios	W_1	W_2	W_3
1	1	0	0
2	0	1	0
3	0	0	1
4	0.5	0.5	0
5	0.5	0	0.5
6	0	0.5	0.5
7	0.25	0.75	0
8	0.25	0	0.75
9	0.75	0	0.25
10	0.75	0.25	0
11	0	0.75	0.25
12	0	0.25	0.75
13	0.33	0.34	0.33
14	0.2	0.2	0.6
15	0.4	0.2	0.4
16	0.2	0.4	0.4
17	0.6	0.2	0.2
18	0.4	0.4	0.2
19	0.2	0.6	0.2

this cDSP the process designer will be able to solve and capture the knowledge associated with the following inverse problem: *Given the microstructure after cooling that best satisfy the end mechanical properties of a new steel product mix, what should be the microstructure factors after rolling and the design and operating set points for cooling that satisfy the requirements identified?*

7 Integrated Solution Space Exploration of Hot Rod Rolling Process Chain Using the Proposed Method

We have exercised 19 different scenarios for both cDSPs in steps 2.1 and 2.2, Table 7. These scenarios are selected based on judgement to effectively capture the design space for exploration in a ternary space with different combination of weights on goals.

We explain the significance of these scenarios using the cDSP for the end product (the cDSP in step 2.1). For the first cDSP, scenarios 1-3 are for a situation where the designer's interest is to achieve the target of on a single goal, i.e., maximizing *YS*, maximizing *TS* or maximizing X_f as closely as possible. For example, the designer's preference in scenario 2 (for cDSP 1) is to achieve only the tensile strength goal. Scenarios 4–6 are for a situation where two goals are given equal preference, and the third goal is not assigned any preference. For example, scenario 4 is a situation where designer's interest is in equally maximizing YS and TS without giving any preference to the X_f goal. Scenarios 7–12 are situations where the designer gives greater preference to one goal, a lesser preference to the second goal and zero preference to the third goal. Scenario 13 is a situation where the designer gives equal preference to all the three goals. Scenarios 14–19 are situations where all the goals are assigned preferences with two of them being the same preference. The exploration of solution space is carried out by exercising the cDSPs for these scenarios and plotting the solution space obtained in a ternary space. The axes of the ternary plots are the weights assigned to each goal and the color contour in the interior is the achieved value of the specific goal that is being addressed. From these plots, we identify feasible solution regions that satisfy our requirements and the associated weights to be assigned to each goal to achieve this solution space. To read more about the creation and interpretation of ternary plots, see Refs. [17] and [42].

7.1 Solution Space Exploration of Step 2.1 *Compromise Decision Support Problem.*

The requirement for the process designer in step 2.1 cDSP is to achieve the goals associated with the mechanical properties of the end rod product. For goal 1, a process designer is interested in maximizing the yield strength. The target value of 330 MPa is specified in the cDSP. On exercising the cDSP and analyzing the solution space in Fig. 6, we see that the red contour region identified by the blue dashed lines satisfy the requirements as closely as possible. The maximum yield strength achieved is 320 MPa and the maximum value has achieved the weight assigned to goal 1 tends to 1. We select the region identified in Fig. 6 as that satisfying the requirement for YS.

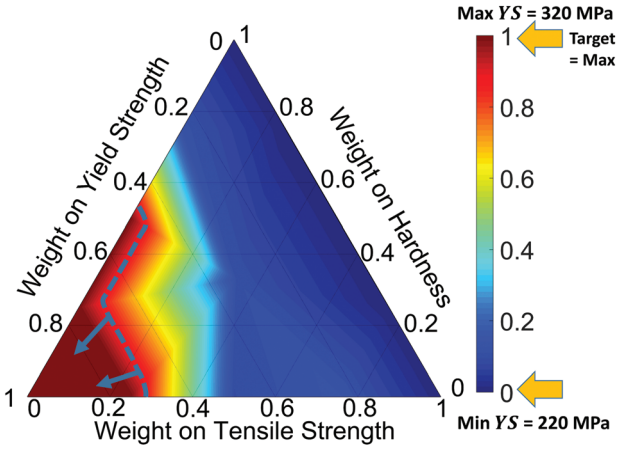

Fig. 6 Ternary plot for goal 1—yield strength

For goal 2, a process designer is interested in maximizing the tensile strength of the product. A target value of 750 MPa is specified for this goal. On analyzing Fig. 7, we observe that the red region marked with the light orange dashed lines satisfies this requirement. The target value of 750 MPa is achieved as we tend to the weight of 1 for the tensile strength goal. However, as the weight on the third goal (hardness) is increased; there is an increase in tensile strength as well. We achieve a value of 750 MPa for tensile strength when the weight on the hardness goal is 1. From this, we can clearly see the forward relationship that hardness and tensile strength hold with respect to the system variables identified.

For goal 3, the process designer is interested in maximizing hardness. The hardness is a function of the ferrite fraction, silicon content and transformational temperature of austenite to ferrite. We assumed a transformation temperature of 700 °C. From Fig. 8, it is clear that the hardness target value of 170 is achieved in the red contour region marked by the white dashed lines. We also observe that the requirement for hardness is achieved in regions

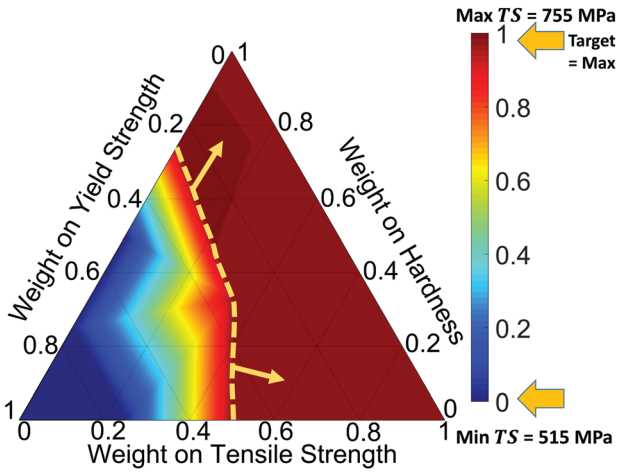

Fig. 7 Ternary plot for goal 2—tensile strength

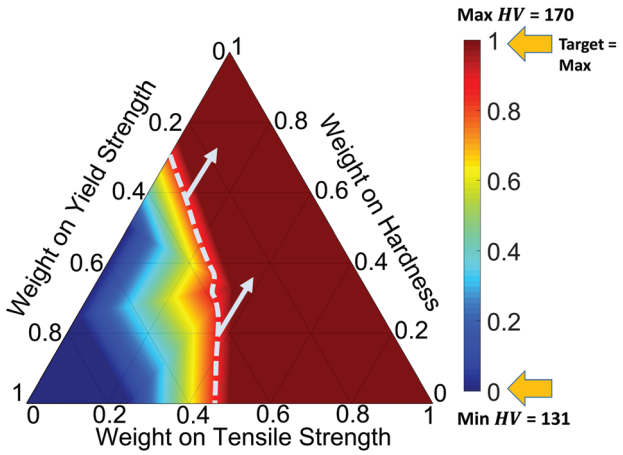

Fig. 8 Ternary plot for goal 3—hardness

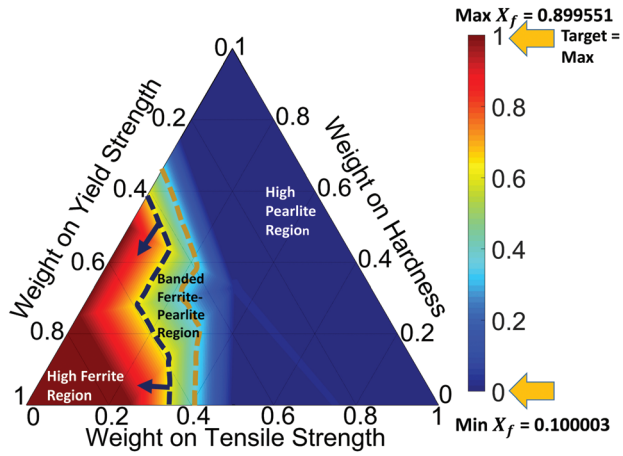

Fig. 10 Ternary plot—ferrite fraction solution space

with high weights for tensile strength confirming the relationship that we saw in Fig. 7.

On carrying out a parametric study with the transformation temperature value, we found that the positive relationship between tensile strength and hardness holds only at high transformation temperatures. At transformation temperatures in the range of 500–550 °C, we see that hardness tends to be greater where there is high yield strength.

Another requirement that must be strictly satisfied is the requirement for minimum impact transition temperature for the rod. From the solution space for the three goals for YS, TS, and *HV*, we check the region where this requirement is satisfied the best. In Fig. 9, the achieved values of impact transition temperature are plotted and we see that the blue contour region marked by two red dashed lines is where the impact transition temperature is minimum. The first red dashed line corresponds to an *ITT* of 0 °C and the second dashed line closer to the blue contour region corresponds to an *ITT* of −66 °C. The minimum ITT is achieved in this region and corresponds to the same region where yield strength is maximized.

On analyzing the results for the mechanical property goals and requirements, we observe that the ferrite fraction system variable plays a key role in defining the mechanical properties. A major requirement is to manage the banded microstructure. In this work, we satisfy this requirement by identifying regions with high ferrite fractions. Hence, we plot the achieved solution space for ferrite fraction with respect to the weights assigned to the three goals in Fig. 10. We see in Fig. 10 that the red contour region marked by the dark blue dashed lines is the region with highest ferrite fraction (near 0.899). The dark blue contour region marked by the dark yellow dashed lines is the region with highest pearlite fraction (ferrite fraction near to 0.1). The region in between these two dashed lines has both ferrite and pearlite. Also, from Fig. 10(*a*), high ferrite fraction supports maximizing yield strength and minimizing impact transition temperature and high pearlite fraction supports maximizing tensile strength and maximizing hardness. The banded microstructure in between satisfies these goals; however, due to the concern about distortions in gear blanks due to these banded structures, the designer must find a region that is either highly ferritic or highly pearlitic in Fig. 10. To come to a decision, we superimpose plots as shown in Fig. 11.

In the superimposed plot, all the regions identified for the mechanical property goals, and the other requirements are combined to identify a single region that satisfies all the requirements, if it exists. If such a region does not exist, the designer must make trade-offs among the conflicting goals. On analyzing Fig. 11, the requirements for maximizing tensile strength and hardness are achieved in the high pearlite fraction region while the requirements for maximizing yield strength and minimizing impact transition temperature are satisfied at the high ferrite fraction region. Hence, the designer is faced with the dilemma of choosing from either the region of high ferrite or high pearlite that satisfies the goals. To make a decision, we first identify some solution points from the superimposed plot and analyze the extent to which the goals are met. We identify 8 solution points A, B, C, D, E, F, G, and H from the ternary space and the results associated with each of these solution points are summarized in Table 8.

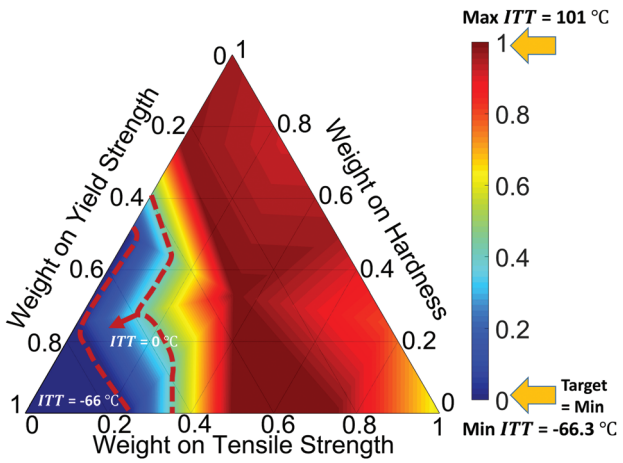

Fig. 9 Ternary plot—ITT solution space

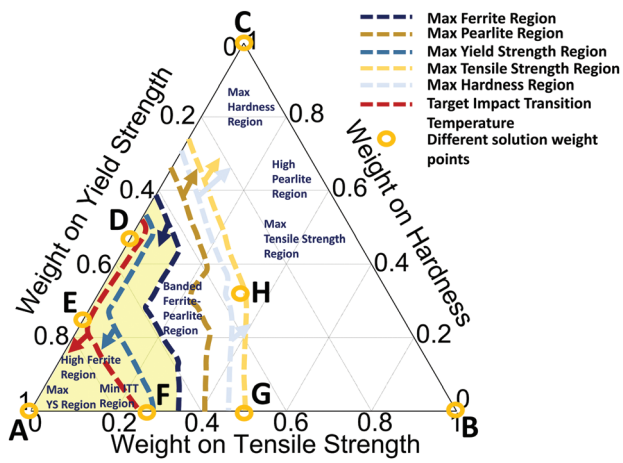

Fig. 11 Superimposed ternary plot

Table 8 Solution points selected

	Microstructure Factors After Cooling				Mechanical Properties of End Rod			
Sol. Pts	D_z μm	X_f	S_0 μm	Mn (%)	YS MPa	TS MPa	HV	ITT°C
A	8	0.9	0.15	1.49	321	516	131	−66
B	8	0.101	0.21	0.7	220	750	169.9	35
C	8	0.1	0.15	0.7	220	749	169.9	94.8
D	8	0.89	0.15	1.5	320	516	131	−66
E	8	0.89	0.15	1.49	320	516	131	−66
F	8	0.89	0.15	1.49	320	516	131	−66
G	8	0.1	0.18	1.5	228	749	169.8	65
H	8	0.113	0.15	1.49	231	749	169.4	100

From Table 8, we see that all the goals are satisfied by minimum values of ferrite grain size D_α and interlamellar spacing S_o. This is a very important information that needs to be communicated to the preceding stages as the requirements from these stages must be to produce a material having these characteristics at the end. On analyzing the impact of ferrite fraction, we see that high yield strength and minimum ITT are satisfied when the ferrite fraction is high, while low yield strength, high ITT, high tensile strength, and high hardness occurs when the ferrite fraction is low (more pearlite). As the pearlite fraction increases, the values of ITT achieved are very high (65–100 °C), which are not acceptable. Hence, we identify regions (the light yellow region in Fig. 11) with a high ferrite fraction, where both yield strength and impact transition temperature requirements are met while compromising on the requirements for tensile strength and hardness. From a design standpoint, the compromise does not severely affect either tensile strength or hardness. Therefore, we choose solution point A having the highest ferrite fraction. Point A achieves a YS of 321 MPa, TS of 516 MPa, *HV* of 131, and ITT of −66 °C.

The solutions for the microstructure space after cooling identified after exploration become the goals for the next cDSP (step 2.2). The target goal for the cDSP for cooling, therefore, is to achieve a minimum ferrite grain size, maximum ferrite fraction, and minimum pearlite interlamellar spacing; target values of 8μm, 0.9 and 0.15 μm, respectively.

7.2 Solution Space Exploration of Step 2.2 *Compromise Decision Support Problem*. The requirement in step 2.2 cDSP is to achieve the targets identified from the first cDSP as closely as possible. For goal 1, the process designer is interested in minimizing ferrite grain size and the target value is 8 μm. On exercising the cDSP and analyzing the solution space for ferrite grain size in Fig. 10, we see that the minimum achieved value of D_α using the current configuration is 10.06 μm. Based on literature study [23,31], we determine that any value less than 15 μm is acceptable as the ferrite grain size after cooling. This updated requirement is met in the region identified by the red dashed lines in Fig. 12. As we move closer to the dark blue contour regions, the requirement for minimum D_α is closest to being satisfied.

For goal 2, the process designer must maximize ferrite fraction to the target value of 0.9. In Fig. 13, we see that the maximum ferrite fraction achieved is around 0.7149. Based on reported ferrite fractions after cooling from the literature [23], we find that any value of the ferrite fraction above 0.68 is acceptable.

The region that satisfies the requirement is marked by the dashed orange line in Fig. 13. As we move toward the red contour region, the maximum ferrite goal is satisfied most closely.

For goal 3, the requirement is to minimize pearlite interlamellar spacing to a target value of 0.15 μm. On analyzing Fig. 14, the minimum value achieved is 0.1497 marked by the blue contour region. Based on reported values of pearlite interlamellar spacing [23], we define that any value less than 0.17 μm is acceptable. This region is marked by the dark blue dashed line in Fig. 14.

Again, to make a design decision, we superimpose all the goals in one superimposed ternary plot, Fig. 15.

In the superimposed ternary plot, the light yellow region satisfies all the requirements. To analyze further we pick six solution points both from within the region identified and outside. Solution points C, D, and E lie within the region that satisfies all the goals in the best possible way. Solution points A, B and F lies outside the region. The results are summarized in Table 9.

On analyzing the results in Table 9, we see that solution point A satisfies the requirement of minimizing ferrite grain size to the greatest extent and this is achieved with a high cooling rate and low value of austenite grain size. This happens because a high cooling rate results in less time for the nuclei to grow before new nuclei are formed resulting in a decrease of average grain size

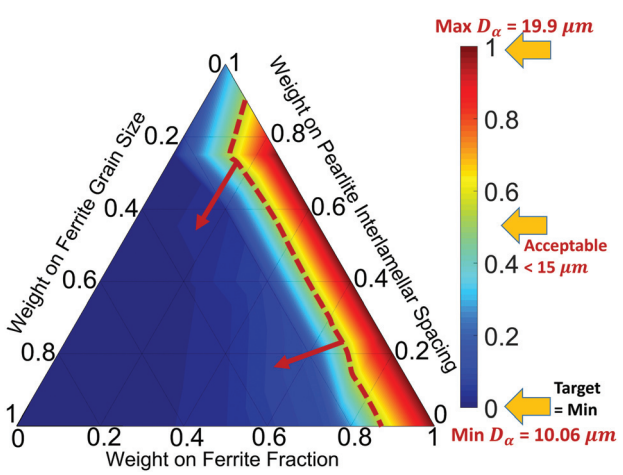

Fig. 12 Ternary plot—ferrite grain size

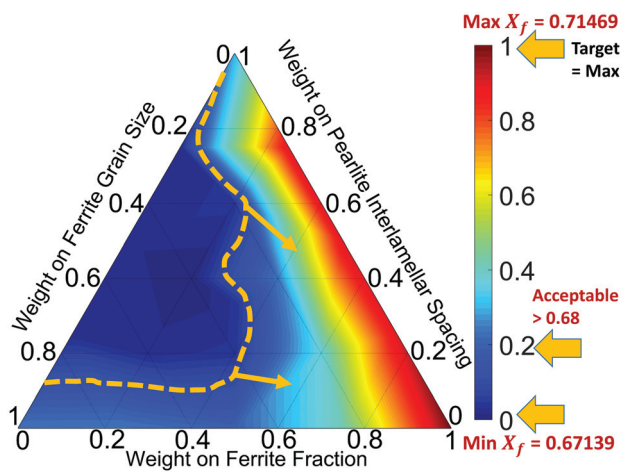

Fig. 13 Ternary plot—ferrite fraction

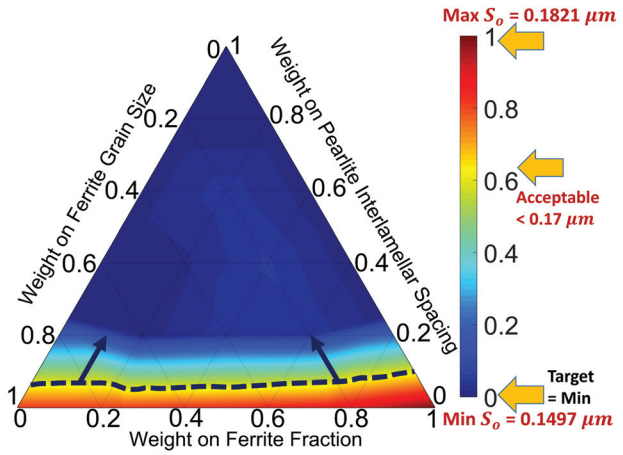

Fig. 14 Ternary plot—pearlite interlamellar spacing

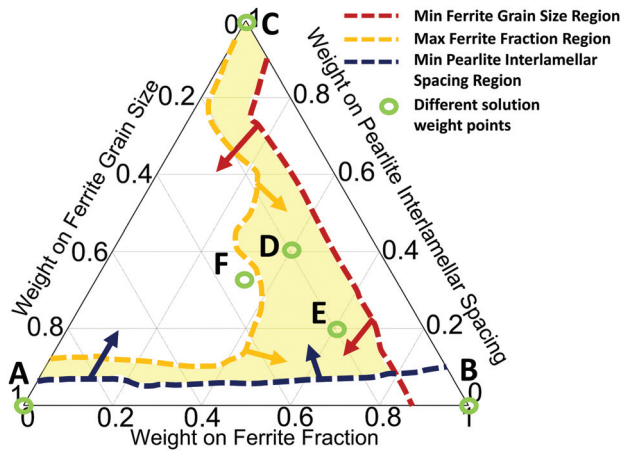

Fig. 15 Superimposed ternary plot for all goals

Table 9 Solution points selected

	Processing (Cooling) and Microstructure Space after Rolling				Microstructure Space after Cooling		
Sol. Pts	***CR*** K/min	***D*** μm	***C*** %	**Mn** %	D_α μm	X_f	S_0 μm
A	99.9	30	0.18	0.7	10.06	0.681	0.176
B	11	74.2	0.18	0.7	19.9	0.714	0.182
C	11	30	0.19	1.02	12.5	0.684	0.149
D	44.4	30	0.18	0.94	10.74	0.681	0.151
E	33.06	30	0.18	0.95	11.05	0.687	0.151
F	70.3	30	0.18	0.93	10.33	0.673	0.151

[27]. This means that there is an increased grain boundary area per volume available for nucleation resulting in more nuclei and thus smaller ferrite grain sizes. Solution point B satisfies the requirement for a high ferrite fraction and this is achieved with a low cooling rate, high austenite grain size and low manganese. The holds true as a low cooling rate favors the growth of allotriomorphic ferrite resulting in the overall growth of ferrite. A high austenite grain size results in an increase in Widmanstatten ferrite, while a low austenite grain size results in an increase in allotriomorphic ferrite. Both these situations need to be considered when studying the effect of austenite grain size on the ferrite fraction. Also, a low manganese content results in less banded microstructure favoring an increase in allotriomorphic ferrite. Solution point C satisfies the requirement for minimum pearlite interlamellar spacing and this is achieved with both low values of cooling rate and austenite grain size. On analyzing all solutions listed in Table 9, we see that solution point D satisfies all the requirements to the extent possible. In Point D the values of a D_α of 10.74 μm, X_f of 0.681 and S_0 of 0.151 μmareachieved. The values for cooling rate, austenite grain size and compositions will act as target goals for the cDSP for the last stage of rolling (cDSP in step 2.3) following a similar format as demonstrated using cDSPs and solution space explorations in steps 2.1 and 2.2.

8 Closing Remarks

In this paper, we present a goal-oriented, inverse method supported by the CEF to achieve the integrated design exploration of the material, product, and manufacturing processes. The method is goal-oriented and inverse because we start with the end mechanical properties of the product and inversely maps the requirements to microstructure and processing spaces of the material to identify multiple solutions that satisfy the requirements. The utility of the proposed method is demonstrated by carrying out the integrated solution space exploration of the processing and microstructure spaces of the rolling and cooling processes to identify *satisficing solutions* that realize the end mechanical properties of the rod product. The method and its application are characterized by a confluence of different disciplines like engineering mechanics, materials science, manufacturing, and systems engineering. The functionalities offered by the method supported by CEF include:

- The method is based on requirements driven, "top-down" design of system and associated subsystems by taking a goal-oriented approach, which is different from the standard practice of bottom-up modeling and design of material and product systems,
- There is the perception of obtaining a satisficing design space across process chains; augmenting the human ability to make design decisions—visualizing a solution space and making logical judgements through trade-offs to identify satisficing solution regions of interest,
- There is the capability to handling 'n' number of design variables—this is an advantage over other design exploration methods like IDEM where there is a limitation on the number of design variables,
- Propagation of end goal requirements (product performance or properties) across a process chain with the designer having the capability to check whether the end goals are actually achievable at previous spaces in their current configuration or not—designer can recommend adjustments in the design space if needed,
- Offers flexibility in design: The capability to define new goals and requirements at each level as the method uses individual cDSPs to facilitate information flow allowing to formulate a design space at each level—advantage over other design exploration methods like IDEM and pyDEM where the design space is defined by mapping from previous spaces [13,15],

- The capability to carry out rapid, integrated design exploration of material and products using simulation models that we accept are typically incomplete and inaccurate,
- The capability to coordinate information and human decision making,
- The CEF offers the capability to prioritize models, input factors, output responses, and computational tools in terms of their value in design, and
- Ensuring feasible design solutions that allow to invest on new complex material systems with confidence.

The proposed method and the concept exploration framework are generic and support the integrated decision-based design of similar manufacturing processes involving the material and product. Given any complex systems problem that involve sequential flow of information across processes/levels, the proposed method has the potential to be applied to support information flow and human decision-making across the processes/levels in order to realize an end goal. Through the proposed method and demonstration carried out in this paper using an industry-inspired problem, we propose an approach for *microstructure-mediated design* by *integrating the design of the material, product, and associated manufacturing processes* involved.

Acknowledgment

The authors thank Tata Consultancy Services Research, Pune for supporting this work (Grant No. 105-373200). Janet K. Allen and Farrokh Mistree gratefully acknowledge financial support from the John and Mary Moore Chair and the L.A. Comp Chair at the University of Oklahoma respectively.

References

[1] Allen, J. K., Panchal, J., Mistree, F., Singh, A. K., and Gautham, B. P., 2015, "Uncertainty Management in the Integrated Realization of Materials and Components," Third World Congress on Integrated Computational Materials Engineering (ICME), p. 339.
[2] McDowell, D. L., Panchal, J., Choi, H.-J., Seepersad, C., Allen, J. K., and Mistree, F., 2009, *Integrated Design of Multiscale, Multifunctional Materials and Products*, Butterworth-Heinemann, Waltham, MA.
[3] Olson, G. B., 1997, "Computational Design of Hierarchically Structured Materials," Science, **277**(5330), pp. 1237–1242.
[4] Horstemeyer, M. F., 2018, *Integrated Computational Materials Engineering (ICME) for Metals: Concepts and Case Studies*, Wiley, Hoboken, NJ.
[5] McDowell, D. L., 2018, "Microstructure-Sensitive Computational Structure-Property Relations in Materials Design," *Computational Materials System Design*, Springer, Cham, pp. 1–25.
[6] Horstemeyer, M. F., 2012, *Integrated Computational Materials Engineering (ICME) for Metals: Using Multiscale Modeling to Invigorate Engineering Design With Science*, Wiley, Hoboken, NJ.
[7] McDowell, D. L., and Kalidindi, S. R., 2016, "The Materials Innovation Ecosystem: A Key Enabler for the Materials Genome Initiative," MRS Bull., **41**(4), pp. 326–337.
[8] Adams, B. L., Kalidindi, S., and Fullwood, D. T., 2013, *Microstructure-Sensitive Design for Performance Optimization*, Butterworth-Heinemann, Waltham, MA.
[9] Kalidindi, S. R., Niezgoda, S. R., Landi, G., Vachhani, S., and Fast, T., 2010, "A Novel Framework for Building Materials Knowledge Systems," Comput. Mater. Continua, **17**(2), pp. 103–125.
[10] Kalidindi, S. R., Niezgoda, S. R., and Salem, A. A., 2011, "Microstructure Informatics Using Higher-Order Statistics and Efficient Data-Mining Protocols," JOM, **63**(4), pp. 34–41.
[11] McDowell, D. L., and Olson, G., 2008, "Concurrent Design of Hierarchical Materials and Structures," *Scientific Modeling and Simulations*, Springer, Dordrecht, The Netherlands, pp. 207–240.
[12] Choi, H.-J., Mcdowell, D. L., Allen, J. K., and Mistree, F., 2008, "An Inductive Design Exploration Method for Hierarchical Systems Design Under Uncertainty," Eng. Optim., **40**(4), pp. 287–307.
[13] Choi, H., McDowell, D. L., Allen, J. K., Rosen, D., and Mistree, F., 2008, "An Inductive Design Exploration Method for Robust Multiscale Materials Design," ASME J. Mech. Des., **130**(3), p. 031402.
[14] Nellippallil, A. B., Mohan, P., Allen, J. K., and Mistree, F., 2018, "Robust Concept Exploration of Materials, Products and Associated Manufacturing Processes," ASME Paper No. DETC2018-85913.
[15] Kern, P. C., Priddy, M. W., Ellis, B. D., and McDowell, D. L., 2017, "pyDEM: A Generalized Implementation of the Inductive Design Exploration Method," Mater. Des., **134**, pp. 293–300.
[16] McDowell, D. L., Choi, H. J., Panchal, J., Austin, R., Allen, J. K., and Mistree, F., 2007, "Plasticity-Related Microstructure-Property Relations for Materials Design," *Key Engineering Materials*, Trans Tech Publications, Zürich, Switzerland, pp. 21–30.
[17] Nellippallil, A. B., Song, K. N., Goh, C.-H., Zagade, P., Gautham, B. P., Allen, J. K., and Mistree, F., 2017, "A Goal-Oriented, Sequential, Inverse Design Method for the Horizontal Integration of a Multi-Stage Hot Rod Rolling System," ASME J. Mech. Des., **139**(3), p. 031403.
[18] Tennyson, G., Shukla, R., Mangal, S., Sachi, S., and Singh, A. K., 2015, "ICME for Process Scale-Up: Importance of Vertical and Horizontal Integration of Models," Third World Congress on Integrated Computational Materials Engineering (ICME 2015), pp. 11–21.
[19] Mistree, F., Hughes, O. F., and Bras, B., 1993, "Compromise Decision Support Problem and the Adaptive Linear Programming Algorithm," Prog. Astronaut. Aeronaut., **150**, pp. 251–290.
[20] Mistree, F., Patel, B., and Vadde, S., 1994, "On Modeling Multiple Objectives and Multi-Level Decisions in Concurrent Design," Adv. Des. Autom., **69**(2), pp. 151–161.
[21] Chen, W., Allen, J. K., and Mistree, F., 1997, "A Robust Concept Exploration Method for Enhancing Productivity in Concurrent Systems Design," Concurrent Eng., **5**(3), pp. 203–217.
[22] Hodgson, P., and Gibbs, R., 1992, "A Mathematical Model to Predict the Mechanical Properties of Hot Rolled C-Mn and Microalloyed Steels," ISIJ Int., **32**(12), pp. 1329–1338.
[23] Kuziak, R., Cheng, Y.-W., Glowacki, M., and Pietrzyk, M., 1997, "Modeling of the Microstructure and Mechanical Properties of Steels During Thermomechanical Processing," National Institute of Standards and Technology, Gaithersburg, MD, NIST Technical Note. 1393.
[24] Majta, J., Kuziak, R., Pietrzyk, M., and Krzton, H., 1996, "Use of the Computer Simulation to Predict Mechanical Properties of C-Mn Steel, After Thermomechanical Processing," J. Mater. Process. Technol., **60**(1–4), pp. 581–588.
[25] Phadke, S., Pauskar, P., and Shivpuri, R., 2004, "Computational Modeling of Phase Transformations and Mechanical Properties During the Cooling of Hot Rolled Rod," J. Mater. Process. Technol., **150**(1–2), pp. 107–115.
[26] Nellippallil, A. B., De, P., Gupta, A., Goyal, S., and Singh, A., 2016, "Hot Rolling of a Non-Heat Treatable Aluminum Alloy: Thermo-Mechanical and Microstructure Evolution Model," Trans. Indian Inst. Met., **70**(5), pp. 1387–1398.
[27] Jägle, E., 2007, "Modelling of Microstructural Banding During Transformations in Steel," Ph. D. dissertation, University of Cambridge, Cambridge, UK.
[28] Shukla, R., Goyal, S., Singh, A. K., Panchal, J. H., Allen, J. K., and Mistree, F., 2015, "Design Exploration for Determining the Set Points of Continuous Casting Operation: An Industrial Application," ASME J. Manuf. Sci. Eng., **137**(3), p. 034503.
[29] Taguchi, G., *Introduction to Quality Engineering, Asian Productivity Organization, 1986, Distributed by the American Supplier Institute*, Quality Resources, Dearborn, MI.
[30] Bras, B., and Mistree, F., 1993, "Robust Design Using Compromise Decision Support Problems," Eng. Optim., **21**(3), pp. 213–239.
[31] Pietrzyk, M., Cser, L., and Lenard, J., 1999, *Mathematical and Physical Simulation of the Properties of Hot Rolled Products*, Elsevier, Kidlington, Oxford.
[32] Wang, R., Nellippallil, A. B., Wang, G., Yan, Y., Allen, J. K., and Mistree, F., 2018, "Systematic Design Space Exploration Using a Template-Based Ontological Method," Adv. Eng. Inf., **36**, pp. 163–177.
[33] Gladman, T., Dulieu, D., and McIvor, I. D., 1977, "Structure/Property Relationships in High-Strength Micro-Alloyed Steels," Conf. Microalloying, **75**, pp. 32–55.
[34] Gladman, T., McIvor, I., and Pickering, F., 1972, "Some Aspects of the Structure-Property Relationships in High-C Ferrite-Pearlite Steels," J. Iron Steel Inst., **210**(12), pp. 916–930.
[35] Yada, H., 1987, "Prediction of Microstructural Changes and Mechanical Properties in Hot Strip Rolling," International Symposium on Accelerated Cooling Rolled Steel, Winnipeg, MB, Canada, Aug. 24–25, pp. 105–119.
[36] Nellippallil, A. B., Allen, J. K., Mistree, F., Vignesh, R., Gautham, B. P., and Singh, A. K., 2017, "A Goal-Oriented, Inverse Decision-Based Design Method to Achieve the Vertical and Horizontal Integration of Models in a Hot-Rod Rolling Process Chain," ASME Paper No. DETC2017-67570.
[37] Robson, J., and Bhadeshia, H., 1997, "Modelling Precipitation Sequences in Power Plant Steels—Part 1: Kinetic Theory," Mater. Sci. Technol., **13**(8), pp. 631–639.
[38] Jones, S., and Bhadeshia, H., 1997, "Kinetics of the Simultaneous Decomposition of Austenite Into Several Transformation Products," Acta Mater., **45**(7), pp. 2911–2920.
[39] Jones, S., and Bhadeshia, H., 1997, "Competitive Formation of Inter-and Intragranularly Nucleated Ferrite," Metall. Mater. Trans. A, **28**(10), pp. 2005–2013.
[40] Jones, S. J., and Bhadeshia, H. K. D. H., 2017, "Program Structure on the Materials Algorithm Project," Materials Algorithms Project Program Library, Feb. 4, 2017, http://www.msm.cam.ac.uk/map/steel/programs/structure.html
[41] Bodnar, R., and Hansen, S., 1994, "Effects of Austenite Grain Size and Cooling Rate on Widmanstätten Ferrite Formation in Low-Alloy Steels," Metall. Mater. Trans. A., **25**(4), pp. 665–675.
[42] Nellippallil, A. B., Song, K. N., Goh, C.-H., Zagade, P., Gautham, B., Allen, J. K., and Mistree, F., 2016, "A Goal Oriented, Sequential Process Design of a Multi-Stage Hot Rod Rolling System," ASME Paper No. DETC2016-59402.